Report:
Installation of a cryogenic station to perform Emission Channeling experiments at low temperature

By: Lígia Amorim
Oriented by:
Professor Luís Peralta - FCUL
Professor Manuel Ribeiro da Sílva IST /CFNUL
Coordination with CERN-ISOLDE: Dr. João Guilherme Correia

30 September 2008

Against my supervisor's advice
I use this first page to release
my humble and rusty musicality of English
repressed throughout this report

I here by thank Professor Peralta
for the greatly appreciated opportunity
that this work has represented to me
and his orientation has provided

I most certainly own the accomplishment
of the global cooling station concept
to Professor Ribeiro da Silva
who has grown me through the process

The sum of all constituent parts
hardly ever equals the whole
thanks to Dr. Guilherme Correia
we have over come our sum

Most parts would not gain
the third dimension up to reality
hadn't it been for Hermano
and his enthusiasm for each

With special acknowledge
not for that that was done,
but for all that I learned
in this simple masters intern

Nothing of what would take place
were not for my family
in their constant support

Nor for Paulo Pereira who
brought a ray of Portuguese sun
every time I got home seek

Thanks
Lígia Amorim

Abstract

The emission channeling (EC) technique is used to determine with high precision the lattice sites of elements/impurities in a single-crystal. With the introduction of a cooling system the EC technique will allow to study the traveling of the impurities in the single-crystal as function of temperature, below room temperature. EC further allows the study of the elements/impurity vibrations and its eventual anisotropy along different lattice orientations.

This report presents the planning and implementation of the cooling station for an existing emission channeling chamber.

Contents

Chapter 1

Motivation

The purpose of this work is to incorporate a cooling station into the already functional emission channelling chamber (EC-chamber) for on-line experiments, allowing measurements from room temperature (300K) down to 50K.

The original EC-chamber is installed on-line with the ISOLDE-CERN beam line and it is used to implant radioactive ions into single-crystal samples. The decay conversion electrons and beta particles emitted by the radioisotopes are collected in a 2D (xz) position sensitive detector. In particular this setup is crucial for the study of ions with a short life time ($T_{\frac{1}{2}} < 6h$) due to the fact that this chamber has both the implantation and detection blocks installed. This setup allows the start of detection just following the implantation, avoiding the loss of an important part of the samples radioactivity time during transfer. Emission channeling is based on pre-existing knowledge of the crystalline structure of the sample and aims to study a specific element type of impurities to follow their particular locations in the lattice. This is achieved by implanting of radioactive ions (probes) into a crystal and by detecting the particles from the decay, through the measurement of the anisotropic emission of charged particles, which channel along the principal axis and planes on crystalline lattices.

The charged particle interacts with the surrounding atoms through Coulomb's potential. The channeling effect depends on the orientation in which it is measured, by measuring several orientations and using triangulation, the preferential location of of the radioactive probes in the lattice site is revealed.

1.1 Channeling:

Studies in channeling techniques are recent, appearing in the mid of the 20th century.

In general channeling can be described as the guiding of a charged particle along a preferential direction of a crystal (represented as a group of charges in a spacial organized structure) due to coulomb interaction of the atom potentials.

For energetic (fast) charged particles the individual coulomb potentials of periodically arranged atoms are seen as one merged continuous potential (through all the crystal) that guides the particle along the lattice's planes or axis as long as its incident angle with that axes/plane remains small. The channeling effect, in single-crystals, occurs when the symmetry of a crystal allows the existence of privileged orientations, axis and planes, in which all atoms are aligned in depth and an energetic beam of charged ions aligned with one of these orientations, feels the coulomb repulsion of the atoms as a channeling force, guiding the charged particles in a trajectory to the depth of the crystal. Channeling techniques are sensitive to the anisotropic distribution of the charged particles inside the crystal, due to the interactions with the lattice and providing in this way information about the crystal internal organization or to the location of impurities/elements inside the lattice. There are two main channeling techniques: first,when the probe charged particle comes from the outside of the crystal (the most common case) the Rutherford backscattering and second, when the probe charged particle comes from the inside of the crystal, Emission Channeling.

The Rutherford backscattering (RBS) technique evaluates the backscattering of a beam of high energetic positive ions, colliding and penetrating on a sample. The backscattering yield allows to determine the elemental composition and concentrations as a function of depth. In RBS channeling the axis and planes are found by the dramatic drop of the measured backscattered yield. When the beam is oriented along different lattice directions the arising channeling effect permits the study of the crystal quality - concentration of defects. If there is an abundance of a certain impurity or defect in the crystal, the method also allows to find out its location by the yield changes and corresponding triangulation for several principal axis.

The other method - EC for the study of elements/impurities in a single-crystall uses the implantation of radioactive ions as probes. The emitted particles, due to the decay of the implanted radioactive isotopes inside the crystal, are collected in a 2D position and energy sensitive detector. This results in an anisotropic intensity distribution of electrons (the current case studies at ISOLDE) out of the crystal and then being detected in the detector, giving 2D patterns. These patterns, measured in x,y within $\pm 3^o$ range, upon fitting to theoretical simulations provide the identification of the the location of the probe in the lattices.

1.2 Refrigeration:

The cooling system will allow the lowering of the sample temperature while measuring the emission channelling effect, giving the possibility of location of an implanted ion at different temperatures. Additionally, besides the low temperature effect on the impurities being a study object by it self, it will reduce the dechanneling effect caused by the lattice disorder and vibration. This effect can be characterized to be used to calibrate the simulations and to measure the vibrations for each direction of the crystal. In future measurements, this method will allow the study of defects and impurities in the materials lattices at low temperatures and consequent phase transitions (a particular case could be the study of phase transitions in super-conductors).

To implement the cooling station closed cycle He refrigerator, it is necessary not only to adapt the station to the chamber, but also to create a mechanism to prevent the condensation of residual gases on the sample surface due to the large difference of temperature between the walls of the chamber, at room temperature, and the low temperature sample holder (around 50K).

The measurement of the sample local temperature in a precise, calibrated and reproducible way is also a very important point to consider in the planning of the experiments, in order to control the temperature conditions of the sample.

1.3 Low temperature and channeling, issues and problems:

The requirement of mobility and compactness of the chamber, (the chamber must be appended for short periods to a beam line nonexclusive to the group) conditioned the choice of a closed cycle He refrigerator with heat dissipation to the atmosphere (in opposition to watter cooling).

The fact that the experiment is carried on a chamber under vacuum drastically reduces the heat propagation eliminating the convection, keeping radiation as the main mechanism and reducing the conduction to the level of the small areas of contact between parts.

There must be a shielding surrounding all the cold circuit, to increase the efficiency of the cooling.

All pieces have must have small size because of the limited access to the inside of the chamber, where the many constituent parts should be assembled.

In addiction there is the need for conduction of the heat all the way from the sample to the cold-finger, without restricting the movements of the sample in the goniometer (needed for the measurements of multiple orientations).

Finally, the experiments require also a precise measurement and control of the temperature of the sample. This implies not only a calibration of the temperature variation of the sample with the temperature of the cold-finger, but also to probe the samples temperature, by placing the sensor diode as close as possible to the sample.

Chapter 2

Principles of refrigeration

As common knowledge, heat is the transfer of energy from one body to another by the mechanism of convection, conduction or radiation caused by a difference in temperature between two bodies.

On a different perspective, refrigeration can be described as a process that removes heat from a system applying it elsewhere to lower the temperature of the first. The generic technological process of deep cooling (obtaining and keeping very low temperatures) is known as cryogenics.

In the first known artificial refrigeration experiment a pump was used to create vacuum in a volume containing ether until it started boiling. As a low boiling temperature liquid the boiling ether absorbed large amount of heat from the surroundings bodies, rapidly lowering its temperature.

57 years after, back in the 1805, a first refrigeration system was designed based on vapor-compression refrigeration cycle. This method consists in the circulation of a refrigerant - gas at room temperature, liquid at low temperature - which absorbs and transmits the heat.

In the first step the refrigerant enters a compressor as gas where it is compressed increasing the temperature in the process.

The compressed heated gas flows then through a condenser where the surrounding walls - working as a temperature reservoir - cool the refrigerant leading to its condensation. The excess heat is dissipated to the outside environment of the condenser.

In the next step, the refrigerant is pushed through an expansion valve, suffering a sudden pressure drop forcing an adiabatic flash evaporation which lowers the temperature of the refrigerant and the walls surrounding it. This is the cold end of the refrigeration system.

Since this time the process has been much developed and improved, still the basic principles of the cryogenic system used for this work in the ISOLDE[1]-CERN[2] are not that different, nor is the system used in this work.

It was already mentioned that the only mean of heat transmission of interest for this system are conduction, to conduct the heat out of the sample holder to the cryogenic cold finger, and radiation, emitted by all objects as function of their temperature. In this work radiation plays an important role, as the walls of the chamber radiate to the interior since they are at room temperature.

2.1 Radiation shielding

According to the Stefan-Boltzmann law $W = \varepsilon(T)\sigma AT^4$ the thermal radiation emitted by a body is proportional to the fourth power of its temperature, T, and to its area, A and surface emissivity, σ in general also dependent of the temperature (and the body's material).

For example, lets consider two black bodies: a sample at constant low temperature T_{sa}, surrounded by a chamber which external surface is in contact with the atmosphere, that works as an heat reservoir at room temperature T_c. The thermal flux needed to maintain the sample temperature, would be negative and depend on the radiation emitted and received by the sample:

$$Q_{provided} = -(Q_{ch\,rad} - Q_{sa\,rad}) \Rightarrow$$
$$Q_{provided} = -\sigma A_{sa}(T_c^4 - T_{sa}^4)$$

[1]"CERN, the European Organization for Nuclear Research, is one of the worlds largest and most respected centres for scientific research. Its business is fundamental physics, finding out what the Universe is made of and how it works. At CERN, the worlds largest and most complex scientific instruments are used to study the basic constituents of matter the fundamental particles. By studying what happens when these particles collide, physicists learn about the laws of Nature." - http://public.web.cern.ch/public/en/About/About-en.html

[2]"The On-Line Isotope Mass Separator ISOLDE is a facility dedicated to the production of a large variety of radioactive ion beams for a great number of different experiments"- (http://isolde.web.cern.ch/ISOLDE/).

Where $Q_{ch\,rad}$ is the heat flux radiated by the chamber, $Q_{sa\,rad}$ is the heat flux radiated by the sample, T_{sa} is the temperature of the sample, and A_{sa} is the superficial area of the sample. This is however an over-simplified equation and there can be differences between this model and the reality. To begin with, the samples and chambers do not behave in general as black bodies, but rather as grey bodies.

A grey body's surface emits diffusely and the monochromatic emissivity is independent of the wavelength, thus the former equation must take into account the surface emissivity factor F_{ij} and the configuration factor F_{conf} of the volumes. The first factor describes the multiple processes of reflection and absorption between the two surfaces and in the simple case of flat parallel plates is given by: $\frac{1}{F_{1-2}} = \frac{1}{\varepsilon_1} + \frac{1}{\varepsilon_2} - 1$ (see also Annex 1). The second factor represents the geometric compatibility of surfaces, as not all radiation leaving one surface intercepts the other surface. In a very rough approximation considering the sample and chamber as parallel flat plates F_{conf} shall be 1.

The thermal flux then becomes :$Q_{provided} = -\sigma F_{ch-sa} A_{sa} (T_{ch}^4 - T_{sa}^4)$ in which the F_{ch-sa} depends of the geometry and emissivity (σ) of the two bodies.

If we consider the existence of thermal shielding between the chamber walls and the sample, we shall have an exchange of energy as illustrated in the diagram of Fig 2.1.

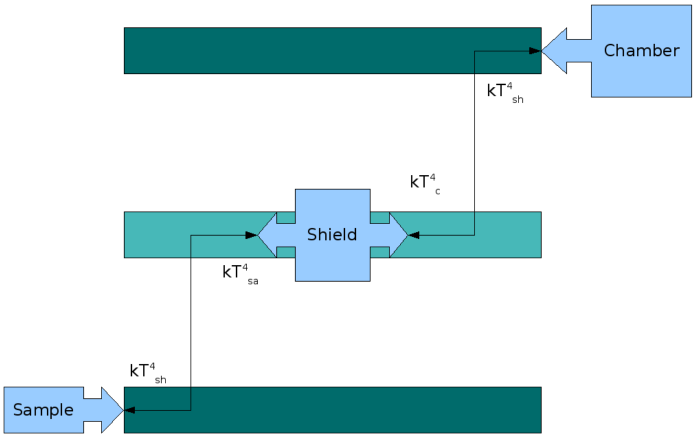

Figure 2.1: Three body radiation flux

Lets study a 3 body system: sample, shield and chamber. The sample is kept at constant temperature of T_{sa}, the chamber is kept at room temperature by the surrounding atmosphere T_c; the bodies are represented as parallel plates ($\frac{1}{F_{1-2}} = \frac{1}{\varepsilon_1} + \frac{1}{\varepsilon_2} - 1$)

The heat flux transfer per unit area. Considering the conservation of energy and all areas equal, without the shield (sh) becomes: $Q_{sa\,ch} = \sigma F_{ch-sa} A (T_{ch}^4 - T_{sa}^4) \Rightarrow (T_{ch}^4 - T_{sa}^4) = \frac{Q_{sa\,ch}}{\sigma F_{ch-sa} A}$ If now we apply the shield between the sample and the chamber, the heat flux is reduced due to the shield emissivity.

$$\begin{cases} Q_{sa\,sh} = (Q_{sh} - Q_{sa}) \\ Q_{sh\,ch} = (Q_{ch} - Q_{sh}) \end{cases} \Rightarrow \quad \begin{cases} Q_{sa\ sh} = \sigma F_{sh-sa} A_{sa} (T_{sh}^4 - T_{sa}^4) \\ Q_{sh\ ch} = \sigma F_{sh-ch} A_{sh} (T_{sh}^4 - T_{ch}^4) \end{cases} \Rightarrow$$

$$\begin{cases} \frac{Q}{A} = F_{sh-sa} \sigma (T_{sh}^4 - T_{sa}^4) \\ \frac{Q}{A} = F_{sh-ch} \sigma (T_{ch}^4 - T_{sh}^4) \end{cases} \Rightarrow \quad T_{ch}^4 - T_{sa}^4 = \frac{Q}{A\sigma} \left(\frac{1}{F_{sh-sa}} + \frac{1}{F_{sh-ch}} \right)$$

Considering again the simplest geometry - three parallel plates, the emissivity factor will be given by:

$$\begin{cases} F_{ch\ sh\ sa} = \frac{1}{\frac{1}{F_{sa-sh}}+\frac{1}{F_{sh-ch}}} \\ F_{ch\ sa} = F_{sa-ch} \end{cases} \Rightarrow \begin{cases} F_{ch\ sh\ sa} = \frac{1}{\left(\frac{1}{\varepsilon_{sa}}+\frac{1}{\varepsilon_{sh}}-1\right)+\left(\frac{1}{\varepsilon_{sh}}+\frac{1}{\varepsilon_{ch}}-1\right)} \\ F_{ch\ sa} = \frac{1}{\left(\frac{1}{\varepsilon_{sa}}+\frac{1}{\varepsilon_{ch}}-1\right)} \end{cases} \Rightarrow$$

$$\begin{cases} F_{ch\ sh\ sa} = \frac{1}{\frac{1}{\varepsilon_{sa}}+\frac{1}{\varepsilon_{ch}}+\frac{2}{\varepsilon_{sh}}-2} \\ F_{ch\ sa} = \frac{1}{(\frac{1}{\varepsilon_{sa}}+\frac{1}{\varepsilon_{ch}}-1)} \end{cases}$$

Considering all surfaces of the same material and with the same surface finish, the equation takes this form:

$$\begin{cases} F_{ch\ sh\ sa} = \frac{1}{\frac{4}{\varepsilon}-2} \\ F_{ch\ sa} = \frac{1}{\frac{2}{\varepsilon}-1} \end{cases} \Rightarrow \frac{F_{ch\ sh\ sa}}{F_{ch\ sa}} = \frac{1}{2} \Rightarrow T_{ch}^4 - T_{sa}^4 = \frac{Q_{sh}F_{ch\ sh\ sa}}{A\sigma} = \frac{Q_{no\ sh}F_{ch\ sa}}{A\sigma} \Rightarrow$$

$$\frac{Q_{sh}}{Q_{no\ sh}} = \frac{1}{2}$$

Thus the location of a shield between the two surfaces results in the reducing of the heat exchange by a factor of 2.

The fact that the sample temperature shall be maintained around 50K and the fact that most of the cooling is obtained by conduction, makes that the installation of shields with mirror surface finish (to have lower absorption factor) surrounding the extent of the cool line is crucial, as it reduces the direct radiation between the chamber at room temperature, the cold line and sample.

In our particular case a good approximation of the shield effect is obtained using the emissivity factor for long concentric cylinders: $\frac{1}{F_{1\ 2}} = \frac{1}{\varepsilon_1} + \frac{A_1}{A_2}\left(\frac{1}{\varepsilon_2} - 1\right)$ Which leads to:

$$\begin{cases} F_{ch\ sh\ sa} = \frac{1}{\frac{1}{F_{sa-sh}}+\frac{1}{F_{sh-ch}}} \\ F_{ch\ sa} = F_{sa-ch} \end{cases} \Rightarrow \begin{cases} F_{ch\ sh\ sa} = \frac{1}{\left(\frac{1}{\varepsilon_{sa}}+\frac{A_{sa}}{A_{sh}}\left(\frac{1}{\varepsilon_{sh}}-1\right)\right)+\left(\frac{1}{\varepsilon_{sh}}+\frac{A_{sh}}{A_{ch}}\left(\frac{1}{\varepsilon_{ch}}-1\right)\right)} \\ F_{ch\ sa} = \frac{1}{\left(\frac{1}{\varepsilon_{sa}}+\frac{A_{sa}}{A_{ch}}\left(\frac{1}{\varepsilon_{ch}}-1\right)\right)} \end{cases}$$

Again considering the surfaces of the same material and surface finish:

$$\begin{cases} F_{ch\ sh\ sa} = \frac{1}{\left(\frac{1}{\varepsilon}+\frac{A_{sa}}{A_{sh}}(\frac{1}{\varepsilon}-1)\right)+\left(\frac{1}{\varepsilon}+\frac{A_{sh}}{A_{ch}}(\frac{1}{\varepsilon}-1)\right)} F_{ch\ sa} = \frac{1}{\left(\frac{1}{\varepsilon}+\frac{A_{sa}}{A_{ch}}(\frac{1}{\varepsilon}-1)\right)} \end{cases} \Rightarrow$$

$$\begin{cases} F_{ch\ sh\ sa} = \frac{1}{\frac{2}{\varepsilon}+\left(\frac{A_{sa}}{A_{sh}}+\frac{A_{sh}}{A_{ch}}\right)(\frac{1}{\varepsilon}-1)} F_{ch\ sa} = \frac{1}{\left(\frac{1}{\varepsilon}+\frac{A_{sa}}{A_{ch}}(\frac{1}{\varepsilon}-1)\right)} \end{cases} \Rightarrow$$

$$\begin{cases} F_{ch\ sh\ sa} = \frac{1}{\frac{2}{\varepsilon}+\frac{A_{sa}}{A_{ch}}\left(\frac{A_{ch}}{A_{sh}}+\frac{A_{sh}}{A_{sa}}\right)(\frac{1}{\varepsilon}-1)} F_{ch\ sa} = \frac{1}{\left(\frac{1}{\varepsilon}+\frac{A_{sa}}{A_{ch}}(\frac{1}{\varepsilon}-1)\right)} \end{cases} \Rightarrow$$

$$\frac{Q_{with\ sh}}{Q_{without\ sh}} = \frac{\frac{1}{\varepsilon}+\frac{A_{sa}}{A_{ch}}\left(\frac{1}{\varepsilon}-1\right)}{\frac{2}{\varepsilon}+\frac{A_{sa}}{A_{ch}}\left(\frac{A_{ch}}{A_{sh}}+\frac{A_{sh}}{A_{sa}}\right)\left(\frac{1}{\varepsilon}-1\right)}$$

Since the sample is surrounded by a shield which is itself contained in the chamber:

$$A_{ch} > A_{sh} \ \wedge \ A_{sh} > A_{sa} \Rightarrow \left(\frac{A_{ch}}{A_{sh}}+\frac{A_{sh}}{A_{sa}}\right) > 2 \Rightarrow \frac{Q_{with\ sh}}{Q_{without\ sh}} < \frac{\frac{1}{\varepsilon}+\frac{A_{sa}}{A_{ch}}\left(\frac{1}{\varepsilon}-1\right)}{\frac{2}{\varepsilon}+2\frac{A_{sa}}{A_{ch}}\left(\frac{1}{\varepsilon}-1\right)} = \frac{1}{2}$$

So by rough calculations we conclude that the shielding can reduce the radiation to a half, hence the importance of the shielding in the cooling station.

2.2 Heat conduction

The conduction, according to Fourier's law is given by $q = -k \oint \frac{dT}{dx} ds$, where q is the heat flux, k is the material's conductivity, T is the temperature, x is the direction perpendicular to the direction of transfer and s is the area through which the heat flows.

The thermal resistance for conduction identifies the impedance felt by the heat flow and in a plane wall is given by $R \equiv \frac{\Delta T}{q} = \frac{1}{Sk}$.

This concept allows the treatment of a multi layer path for conduction, since the resistance is addictive: $R = \sum R_i \Rightarrow q = \frac{\Delta T}{\sum \frac{\Delta x}{k_i S}}$

It follow that the problem is not mainingly the elements conductivity, because the significant value is dependent on the size of each layer. In general the fact that it is a multi-layer system does not imply directly the lost of conduction, because if we use for all layers the same material the result will be the same as of one layer. $q = \frac{\Delta T}{\sum \frac{\Delta x}{kS}} = \frac{\Delta T k S}{\Delta x}$

The main issue is the thermal contact resistance, due to the roughness of the layers and existence of gaps between them (appendix b thermal resistance). As presented in the table of conductivity -appendix b- despite temperature variation (which is considered insignificant for the matter), the presence of air in between the various parts could reduce significatively the conduction effect.

In our case, working in high vacuum conditions, the solution is to reduce the roughness and increase the flatness of the surfaces, and to create assembling methods that can force a better the contact.

2.3 Heat transmition

Summarizing, there are SEVERAL IMPORTANT POINTS to consider in the design of the installation:

- There must be a shield surrounding all the extent of the cold circuit to increase the efficiency of the cooling.
- The conductivity values of the materials to use in the conduction path must be taken into account, as other important technological parameters as welding and polishing techniques.
- There is the need for conduction of the heat all the way from the sample to the cold-finger without restricting the movements of the goniometer sample holder (each measurement can require multiple orientations).
- The connection of the pieces has also to be optimized, to reduce the thermal contact resistance.
- All cryostat parts shall have limited size to ease the access to the inside of the chamber where many constituent parts should be assembled.
- To conduct the experiments it is required a precise measurement and control of the sample temperature. This implies not only a calibration of the sample temperature variation with the cold-finger temperature, but also the fitting of the sample the closest possible to the temperature measuring diode.

2.4 Principles of the device

The general concept behind the refrigeration is the Carnot cycle, using a piston and compressed gas. Considering only the system cylinder with a piston and compressor with refrigerant gas (with two interences of gas, one more pressurized than the other), the Carnot cycle has the following main steps:

- With the piston down and the high pressure entry of the compressor opened the piston is moved up, forcing the entrance of the refrigerating gas. The work done against the piston (forced by the pressure of the gas) results in a isothermal expansion.
- Closing the high pressure and opening the low pressure entry of the compressor the gas expands and so lowers the temperature in an adiabatic expansion.
- The difference of temperature causes a heat flux between the gas and the walls of the cylinder. This process lowers the temperature of the cylinder and increases that of the gas.
- The piston is lowered pushing the gas out to the low pressure entry of the compressor. The work done by the piston against the gas can be seen as an isothermal compression.

- opening the high pressure and closing the low pressure entry of the compressor we recover the initial state closing the cycle through an adiabatic compression.

The process can better illustrated by a plot of pressure as function of the volume (2.2).

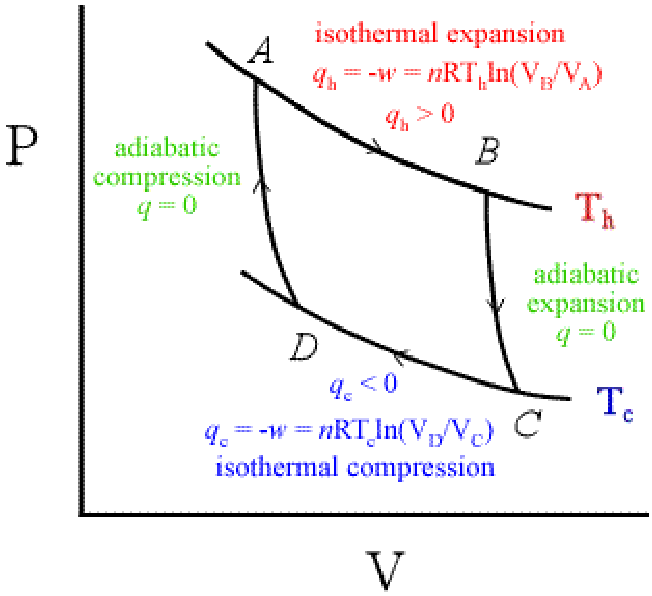

Figure 2.2: Carnot Cycle

In the case of this particular station a regenerator is used to better recover the heat from the walls.

The regenerator will be cooled by the out going gas, when it has already cooled the walls but is still below room temperature. Afterwards, the incoming gas will go through the regenerator, increasing the cooling before it enters the cylinder and the all process begins again. This way lower temperatures are reached, and the losses are lowered, since the compressor is at room temperature.

Addictionly the regenerator is build in the piston and the entrance of gas is made through the piston into the opposite side of the cylinder to that of the cooling load. Once the compressed gas enters the upper part of the cylinder, it will flow through the regenerator into the load only due to its pressure. It will also be driven back by the pressure differential when the other entry of the compressor is opened the piston is now considered a "displacer" producing no work.

This type of system can get down to the 30K. However to obtain lower temperatures, you need to apply the Carnot cycle more than once and so in this cooling station there are two stages of Carnot cycles working inside the cold-finger, reaching in such way 7-10K minimum.

2.5 Cooling station:

The cooling station consists of three parts:

- The compressor, a large block that produces the power work needed to keep an entry at low pressure and one at high pressure (2.3 a).
- The cold finger, a device in which the cycle of helium will take place and so all the process of cooling (2.3 b).
- A resistance is applied around the cold finger to control the temperature, since the cycles lead allways decreases temperature with a constant duty cycle. A diode is secured to the cold-finger as the reference temperature gauge.
- The controller calculates the current needed to heat the resistance in order to achieved a set point temperature in the reference diode (2.3 c).

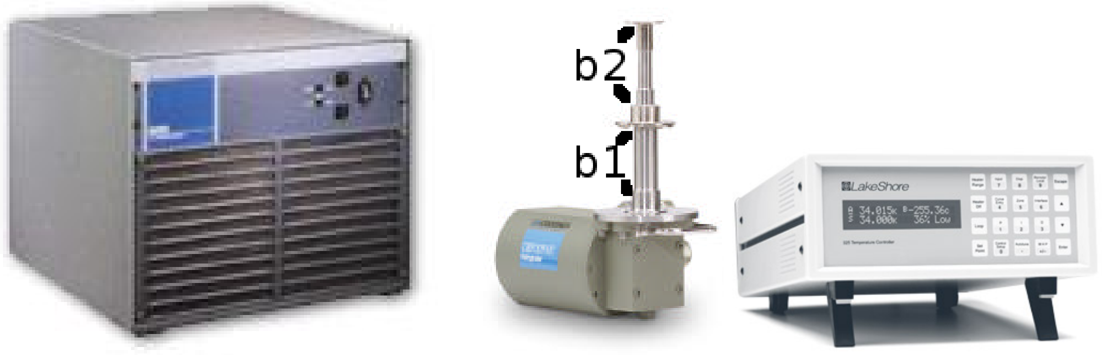

(a) Helium compressor (b) Cryogenic refrigerator head (c) Process controller

Figure 2.3: Cooling blocks

2.6 Cold-Finger:

The cold finger has three zones:

- The zone of lowest temperature where it reaches the 7-10K is at the extremity of the finger, where the second Carnot cycle takes place (b2).
- The zone of the first Carnot cycle that reaches around 30k (b1).
- The room temperature zone (the olive green zone in 2.3 b) that is connected with the compressors entries through flexible tubing. It also fully supports the cold-finger, mechanically attached to the chamber flange.

The aim of this project is to get the lowest temperature possible in the sample. In order to obtain such low temperatures in the sample the starting point of the conducting path is mounted in contact with the second Carnot cycle zone (b2).

The sample shield is attached to the first cycle zone (b1), keeping its temperature low and diminishing the radiation into the main conduction path.

The concept design ensures that both paths (conducting and shielding) do not cross each other, nor the chamber's walls, which remain at room temperature. If the paths would cross that would allow conduction of heat and either raise the radiation (if the shielding touches the chamber and heats up) or lower the conduction of heat (if the conduction path meets the shielding path then the conduction of heat into the cold finger would be divide by both paths).

2.7 Compressor:

The compressor has the cycle from the gas entry to the pressurized exit. The helium flowing through its lower pressure entry is sprayed with oil. The oil is used because it has higher specific heat than the helium and so the heat increase due to compression will be received mainly by the oil that is collected posteriorly. Then the compression takes place in the compression pump and the mixture gas and oil is directed to a heat exchanger that will collect the heat caused by the compression (at least the difference between the temperature of the mixture and room temperature).

After cooling to room temperature the gas is separated from the oil and is ready to be pushed to exit at the high pressure entry of the compressor.

Since the compressor block must be moved with the chamber, it was chosen to be air-cooled, avoiding watter and pipes.

Chapter 3

General view of the EC chamber

3.1 Blocks schema:

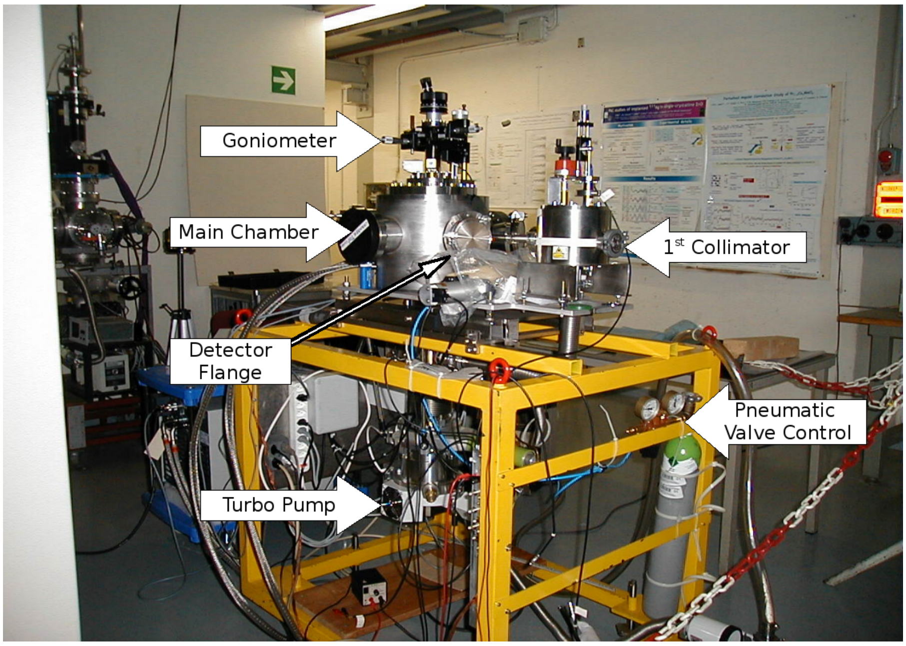

Figure 3.1: The global experiment setup picture

The EC-chamber assembly is composed of the following parts:

- Goniometer - controls the position and orientation of a sample. It is mounted in a special flange on the chamber top and reaches the center of the chamber with an arm with the sample holder at the end.
- Vacuum circuit- consists of a primary plus a turbo pump connected to the bottom flange of the chamber. As standard all the chamber flanges are CF with copper O-rings. For easy operation the most usually opened flanges can be sealed with viton O-rings.
- Collimators - there are two collimators, the first one collimates the beam before entering the main chamber and the second one is located (∅1mm) is in the main chamber just before the sample space.
- laser alignment- a laser device with 3 movements (z, rotation and tilt) is used to align the collimators, thermal shield, sample holder and Faraday cup along the same optical axis of the chamber. The laser device is mounted in the first collimator chamber.
- Faraday cup - a copper cup is used as a Faraday cup, a trap for charged particles to measure the current of the beam and calculate the rate of implanted ions. The movable Faraday cup is inserted in the chamber from a side flange and positioned behind the goniometer sample holder. It can be active only when the goniometer is recoiled to its uppermost position.

- detector - the detector block (detector chamber, xy solid state detector and shutoff valve) is mounted in a flange at 17 degrees with the beam line. A second spare detector flange at 30 is available on the left side of the chamber.

The figures 3.1 and 3.1 shows the schematic design of the chamber.

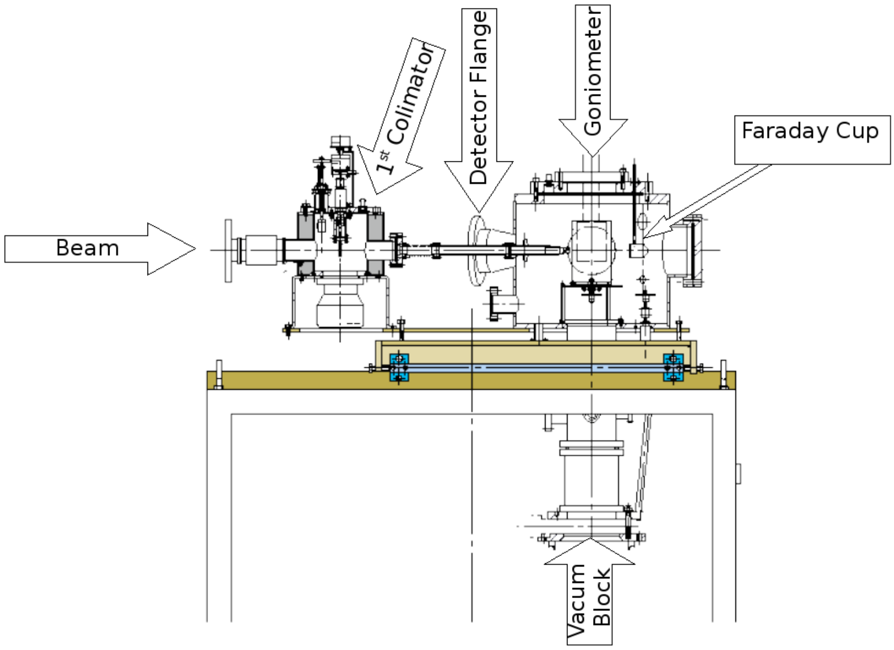

Figure 3.2: The global lateral chamber setup

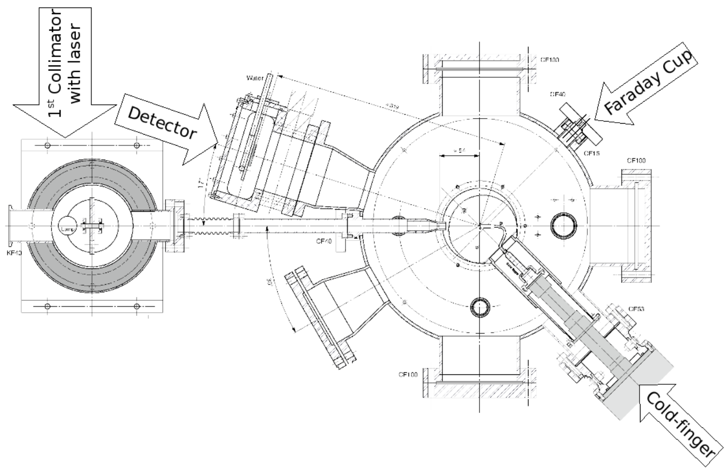

Figure 3.3: The global top chamber setup

3.2 Goniometer schema:

The goniometer is mounted on the top of a non-standard CF200 flange with vacuum tight electrical feedthrougs. The goniometer is a Vacuum Generators mounted on a xyz platform and with a 2 axis rotation sample holder. The max z movement it allows is about 50mm, the rotation in the xy plane is 360 degrees (M1) and the rotation perpendicular to on the plane of the sample holder (M2) is of 180 degrees ([-90,90]).

For the emission channeling measurements the sample axis must be centred with the detector. Adjustments of z can be of the order of 30mm.

The sample holder has two thermocouples and a heating element allowing annealing up to 1200K.

Figure 3.4: A goniometer, much like the one used (or so we wished)

3.3 Vacuum circuit schema:

The basic vacuum block is as shown in figure 3.5.

Through valves the primary pump is connected directly to the chamber. This setup allows to make rough

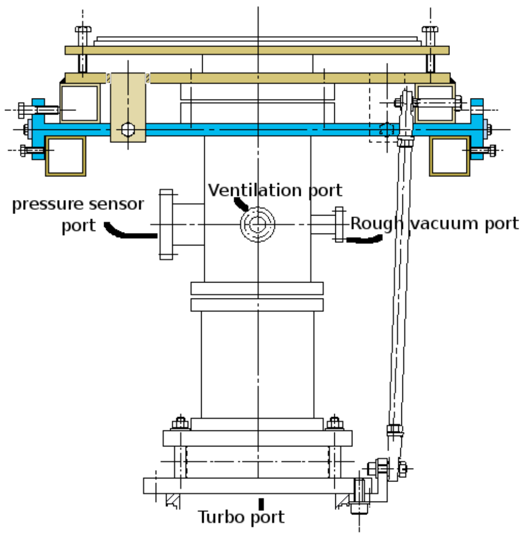

Figure 3.5: The vacuum schema

vacuum in the chamber with the turbo valve closed. A valve gate is mounted between the chamber and the turbo pump so the chamber can be vented and opened without shutting down the turbo. The venting is done by a special venting valve mounted in the vacuum block. The pumping system can keep the chamber under a vacuum of the order of 2×10^{-7} mbar.

3.4 Laser alignment and Faraday cup schema:

The laser is used to align the chamber axis with the beam line and with the sample holder. It is located inside the 1st collimator chamber, as shown in the figure 3.6. It is manipulated from the outside, with a precision endless screw to position it on, or remove it from, the beam path.

The Faraday cup is used when the goniometer is out off the beam to evaluate the beam intensity and

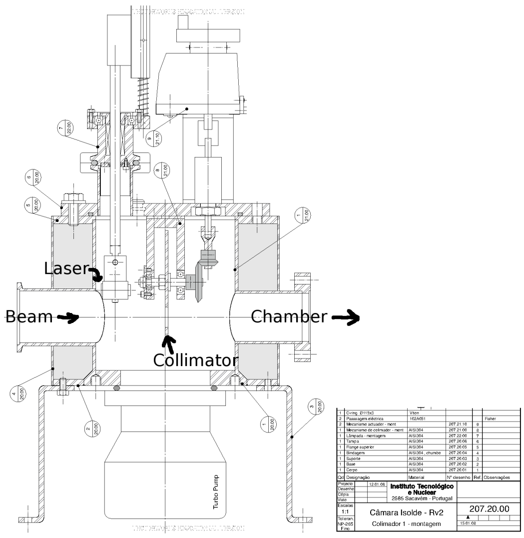

Figure 3.6: The laser in the colimator1 chamber

to optimize the beam focusing. The radioactive beam is created by colliding 1GeV protons into a target; the target nuclei are broken to exited radioisotopes, then freed and accelerated. To focused and direct the beam to the on-line setup, there is no need for radioactivity. So stable isotopes are used to do beam adjustments.

The positive ions of the beam recombine with the electrons, when colliding with the metal material (Faraday cup). Using a picoamperimeter, a positive current is measured that is proportional to the rate of ions implanted. Measuring the current and integrating through the time of the implantation one obtains the quantity of implanted atoms.

The ions when colliding, bring so much energy that the atomic electrons of the Faraday cup are released off the material, resulting in a missleading value of current. For this reason a repeler is mounted in the entrance of the Faraday cup. The repeler, a circular negatively charged plate, sends back the electrons ($\sim 10^2$eV) into the Faraday cup.

A round collimator is mounted at the entrance of the Farday cup. The measurement of the current on it provides further information for the alignment of the beam.

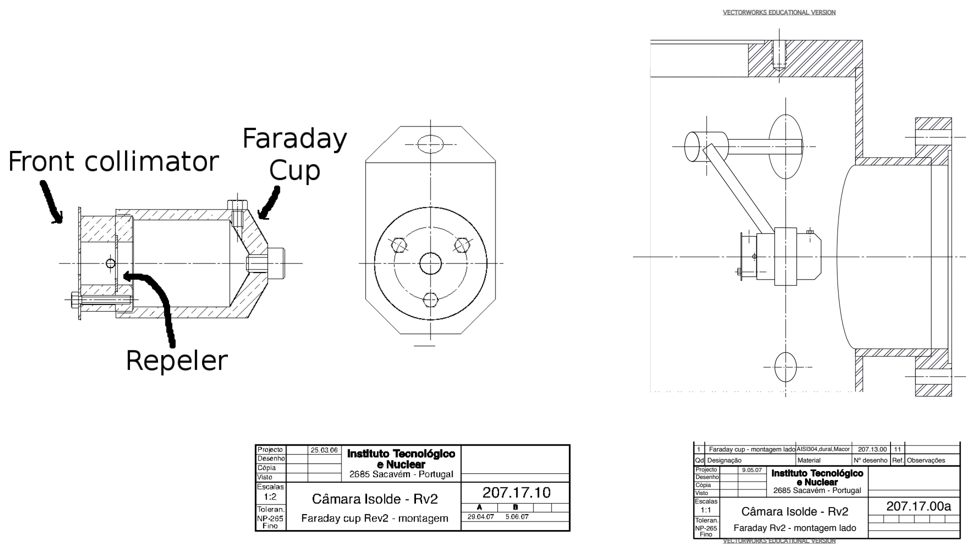

(a) Faraday cup parts

(b) Faraday cup mounted

Figure 3.7: Faraday cup

Chapter 4

Concept of the cooling system

The mounting of the cold-finger into the chamber required a special flange, converting the cold-finger 102mm flange with Imperial screw holes into a CF63 with Metric screwing. (Fig. 4.1)

The feedthroughs are used to connect the cables from the inside of the chamber to the out side.

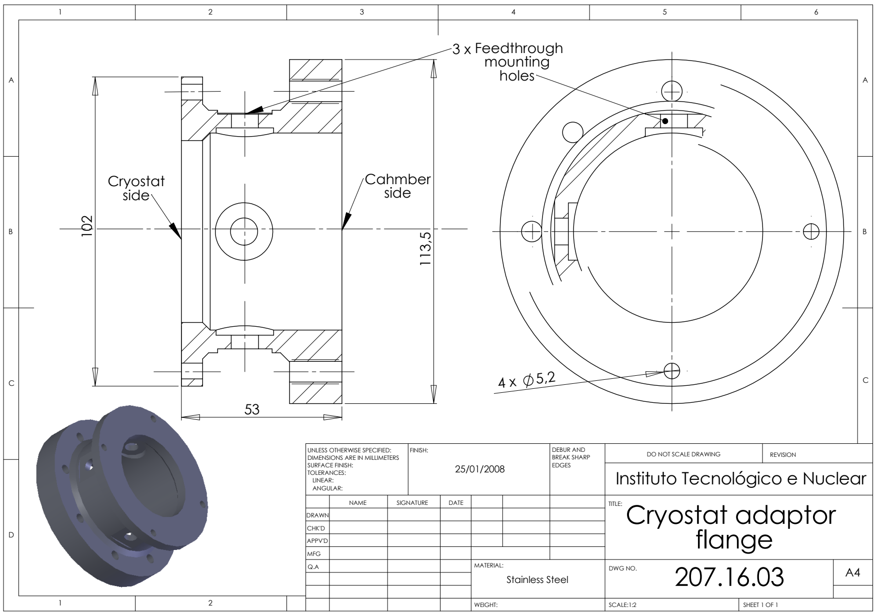

Figure 4.1: The cryostat adaptor flange

All cables to connect the resistance and diodes to the controller had to be made.

4.1 Compressor

The compressor is very large and heavy (40kg). For this reason and due to the need for it to accompany the movable chamber, it is put into a strong four wheels platform (Fig-4.2). There was the simplest possibility of just attaching 4 wheels into the compressors bottom. But once again the screws had to be Imperial standard what was far more complicated and expensive to mount.

4.2 Temperature Control

The cold-finger has only one way of working at full duty cycle. To control the temperature a resistance had to be glued to the first stage of the cold-finger, in order to be used as heater (Fig.4.3). The resistance has to make as much contact as possible, because once again conduction is the only method of heat dissipation available

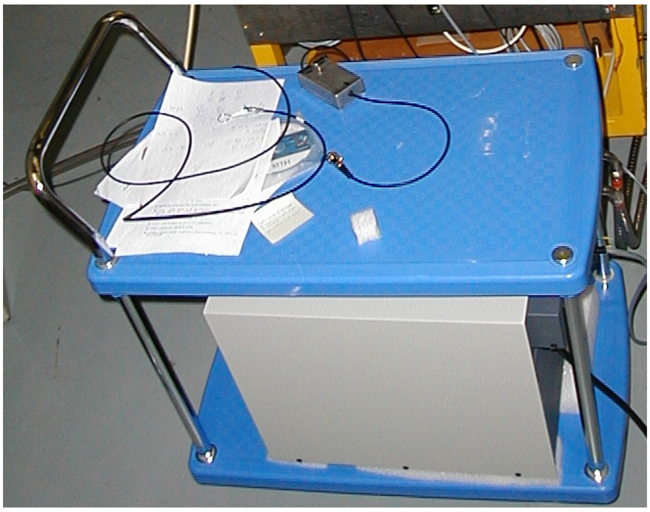

Figure 4.2: The He compressor trolley

in the vacuum chamber with enough power. Then a diode was attached to the first stage of the cold-finger, to measure its temperature. Its position in the first stage of the cold-finger is to optimize the work of the controller. It is used to correct the current needed to warm up to a certain temperature where the response of the system is faster. This is obtain reducing the distance between the heat source and the measurement.Together, both the resistance and the diode are connected through the feedthroughs to the controller to the outside of the chamber.

For better understanding of the temperature gradients in the chamber, an additional diode was placed

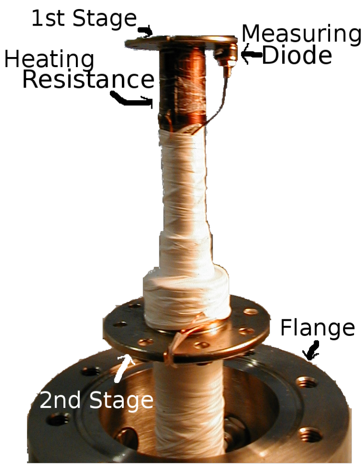

Figure 4.3: Cryostat cold-finger with the diode and the heater

in the main shielding. In this way the radiation shield temperature can be monitored, giving an idea of the running conditions. This is also usefull, because if any accidental contact occurs between the flexible conduction path and the shielding, the temperature of the first would decrease and the temperature of the second would rise extremely rapid.

The controller allows the monitoring of only 2 diodes, being one of them the reference diode. For this reason a switch was mounted that connects to the controller either the shield or the sample measuring diodes upon selection. The switch can be seen on the top of the trolley block as the small metal box (Fig.4.2).

Chapter 5

Connecting the cryogenic station to the goniometer

To connect the cooling station we had to pay attention to several problems:

1. The design of the sample holder and its interface with the thermal conducting path.
2. The need for a flexible design for the conduction path.
3. The design of the plug to connect the cold-finger extremity to the conduction path.
4. The construction of a shield that would allow the movements of the goniometer and still covers all the conduction path and fit the chamber accesses.
5. The shielding also must conduct the cold through its path, and so the mounting process must allow planar contact surfaces.

5.1 Interface between cold-finger and sample:

To cool the sample the heat must be conducted to the cold-finger. In order to avoid cooling the full goniometer sample holder, which is not conceived as a cryogenic system, a small sample holder was conceived and a 0.2mm capton foil isolates both.

The sample holder is positioned in front of the goniometer but the conduction to the cold-finger must be done from the opposite side. This prevents the cooling parts from ever shadowing the sample in relation to the detector, but it also implies that the connection from the sample holder to the conduction path must be made out of the goniometer sample holder space (by its side Fig.5.1).

In fig.5.1 the darker part represents the goniometer sample holder, resistance and all the rotation mechanism a side or it would be much thicker.

The aluminum part is the sample holder (Fig.5.2 a). The choice of aluminum for the sample holder was mainly due to two characteristics of the material. Due to its reduced weight it does not represent a problem for the goniometers rotation mechanism, and its the high value of conductivity, allied with the fact that when the aluminum oxidates, creating a surface layer of alumina, it maintains, for low temperatures, high conductivity values (Table.B) which is of most importance.

The copper piece (copper braid support in Fig.5.2 b) is the connector of the sample holder to the cold path. The copper braid support had to be made out from two pieces, the arm and the base welded together, for this reason the aluminum would represent a technical problem. The high conductivity of copper is altered (lowered) by its oxidation and so the pieces made of copper were gold plated (with $\sim 1\mu m$).

To answer the problem referred in the second point the cold is transmitted by a copper braid (5.3). This allows a flexible and extendible, access to the cold-finger and since it is made of copper, the conductivity is also high. The copper braid is welded and crimped in the arm of its support.

The third point is a problem of optimization, the mounting process of the cold-finger connection to the rest of the conduction path inside the chamber must be easy and practical due to the limited space. A large screw (cold-finger edge) is mounted at the end of the cold-finger. This way, to attach the copper braid tip to the screw a nut is mounted in the end of the conduction path(Fig.5.4).

The twisting of the nut when applied in the screw must not twist the copper braid. For this reason the copper braid tip (Fig. 5.2 b) is independent from the nut. The copper braid is weld and crimped to the tip. All together the conduction path is mounted as illustrated in the figure 5.5 b).

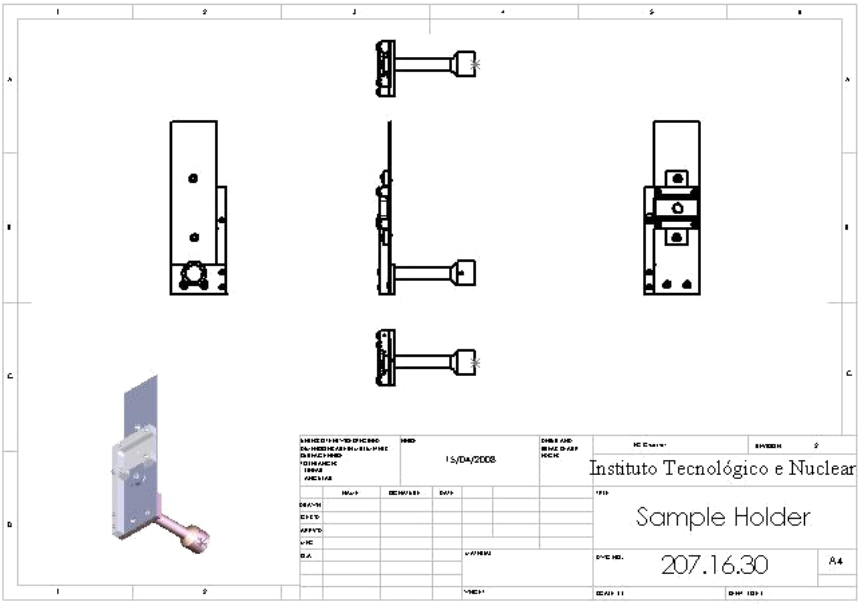

Figure 5.1: Sample holder and copper braid support

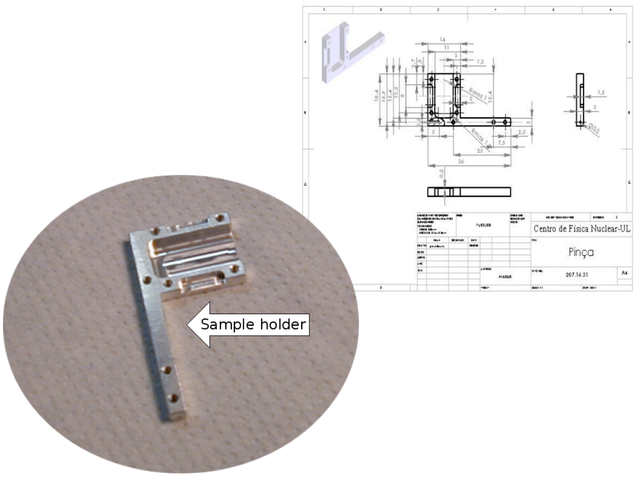

(a) Sample holder

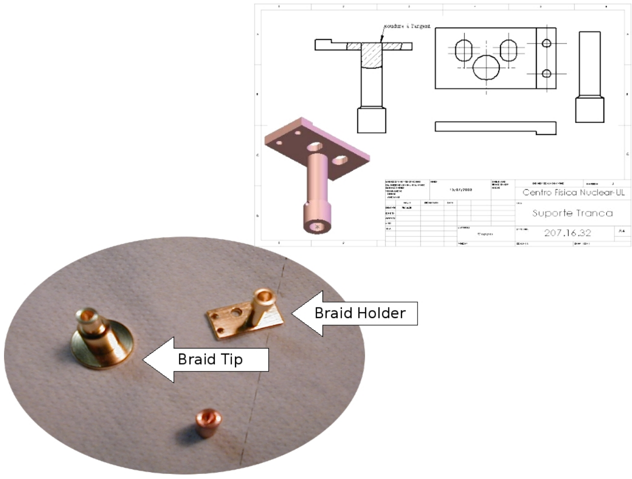

(b) Copper braid support

Figure 5.2: Sample holder and copper braid support designs

5.2 Thermal shielding

To solve the problem, arising in the forth point above, various geometries were tested in cad design for the main shielding.

The first idea was to use a cylinder, but the fact that this main central shield had to connect to a perpendicular shield coming from the cold-finger second stage made it somewhat hard to design. The cylinder would represent the problem of building a piece that could be held against the cylinder.

In the end to force a good contact the better way is to use a thread and a screw, which is difficult to machine on a cylindrical surface. Considering polynomial prisms that could fit through the chambers flanges, it was found that the goniometers sample holder would hit the shield walls when moving M1 and M2 rotation axis.

The need for both, a planar surface and a cylindrical geometry where then combined. For manufacturing purposes the face was reduced to a cut where a square piece with a circular thread is weld (Fig.5.6).

The shielding path, from the main shielding to the cold-finger first cycle, is divided in two parts. One part, the first shield, is connected permanently to the cold-finger first stage with normal screws and shields its all second stage (Fig.5.7). It has a screw tip where the second part connects.

Figure 5.3: Copper braid

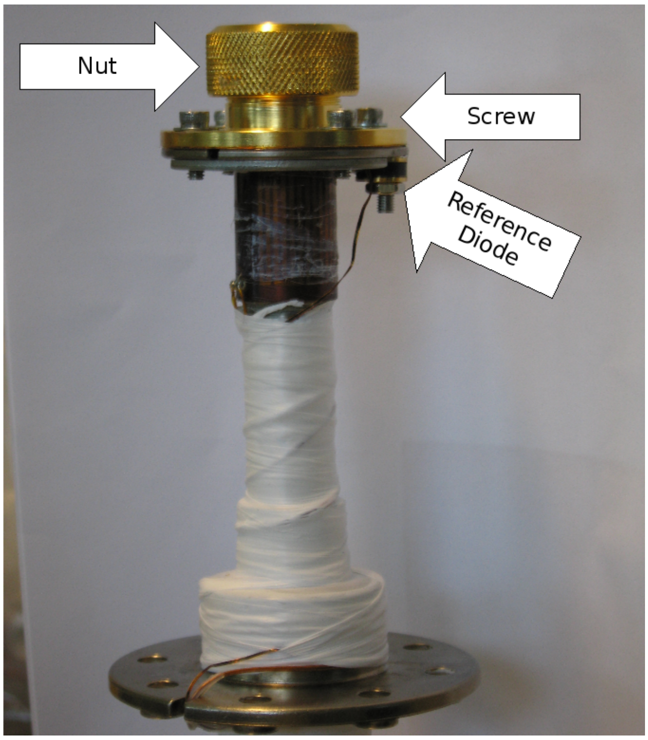

Figure 5.4: Cold-finger edge

The second part is larger and has thread inside to attach to the 1st shield. It is a large nut and so is able to twist its way up and down the 1st shield. In its lower position it covers the whole first shield, to release the chambers space(very important to mount the conduction path). To connect to the main shield it slides/twists through the 1st shield, keeping a small part attached to the 1st shield. The other end connets with the main shield with a screw tip.(Fig.5.7 b and c)

5.3 Cryogenic station installation procedure

There are few steps to install the station:

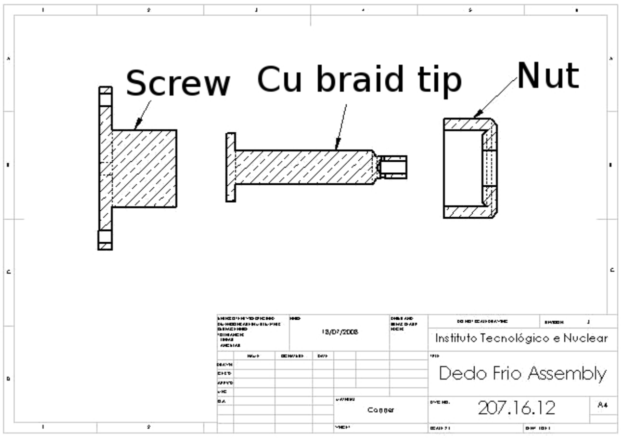

(a) Cold-finger connectors

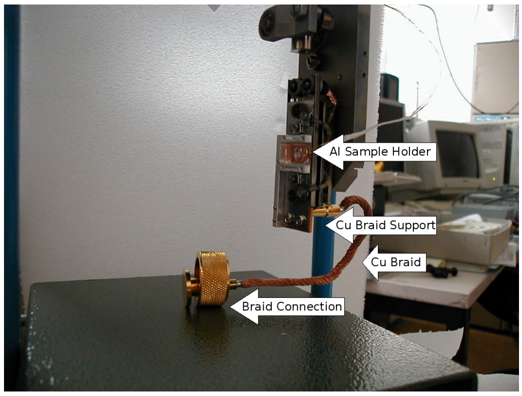

(b) Conduction path mounted

Figure 5.5: Conduction path

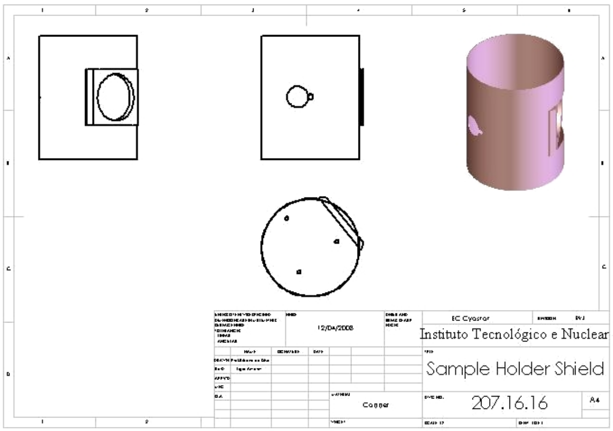

(a) Main shield schema

(b) Main shield picture

Figure 5.6: Main shielding

- Firstly the cold-finger is prepared with the resistance, the diode, the first shield and the cold-finger end. (Fig.5.7 c)
- Secondly the cold-finger is mounted on the chamber, using the connecting flange. (Fig.5.8 a)
- Thirdly the goniometer is prepared with the sample holder and all the conduction path, up to the nut. (Fig.5.8 b)
- Fourthly the main shield is inserted in the chamber, the access is made by the upper flange. The goniometer is inserted into the chamber, the conduction path is fished out of the main shield and connected to the cold finger. (Fig.5.8 c)
- Finally all connections done the second shield slides out of the first shield and twists into the main shield. (Fig.5.8 d)

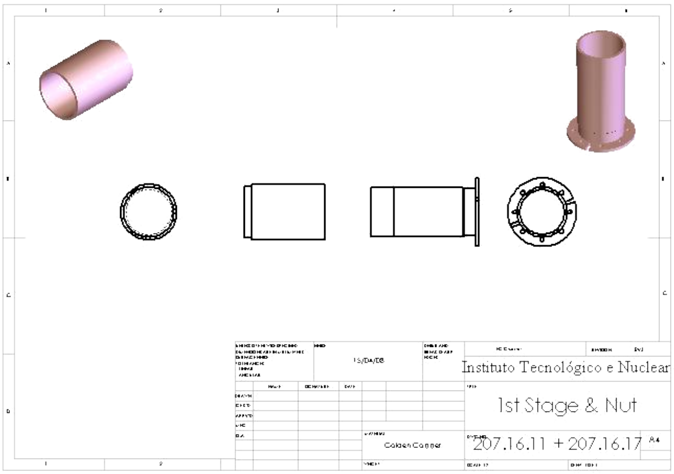

(a) Shielding path schema

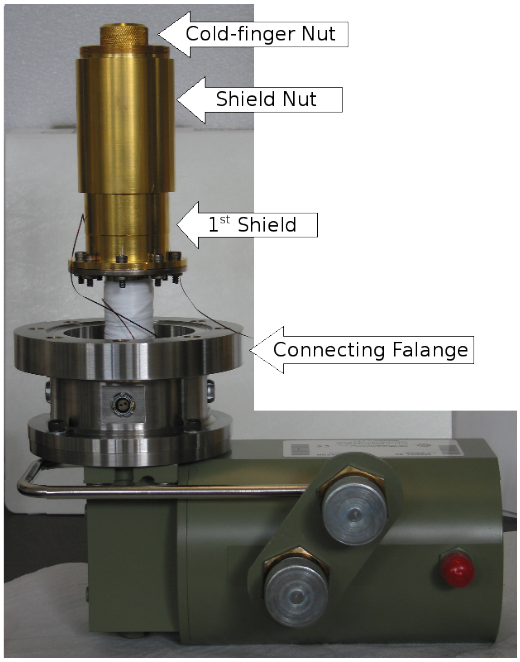

(b) Shielding picture

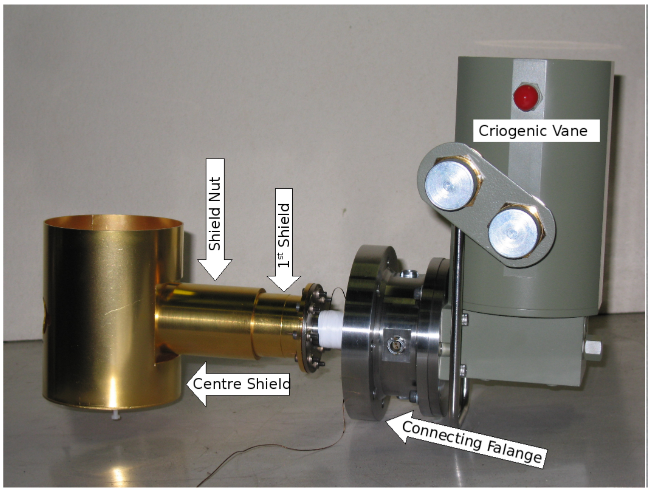

(c) Shielding path schema

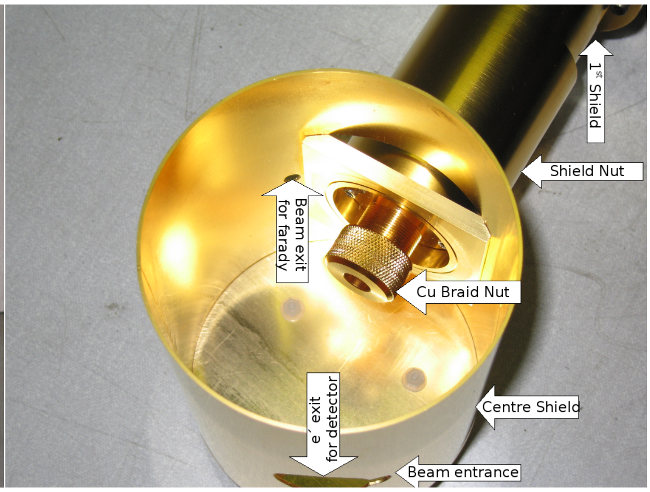

(d) Shielding path picture

Figure 5.7: Shielding path

In conclusion the schema Fig. 5.9 describes the cooling station designed and the resulting heat flux (as in fig.2.1) between the three main subjects, the chamber, the shielding and the sample.

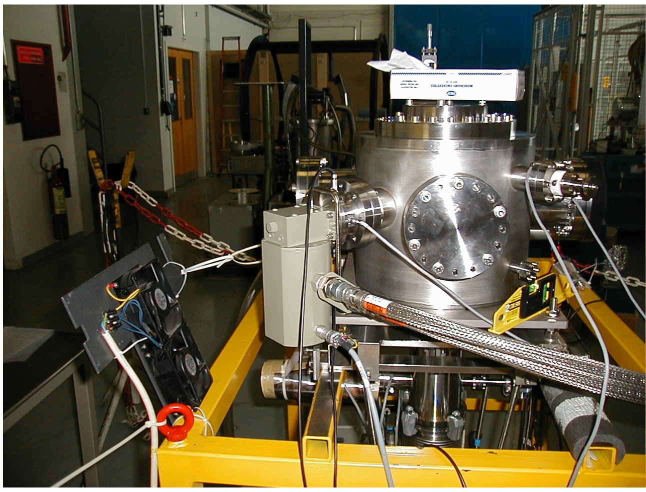

(a) Cold-finger in the chamber

(b) Mounting the conduction path in the goniometer

(c) Copper braid fished out of the main shielding

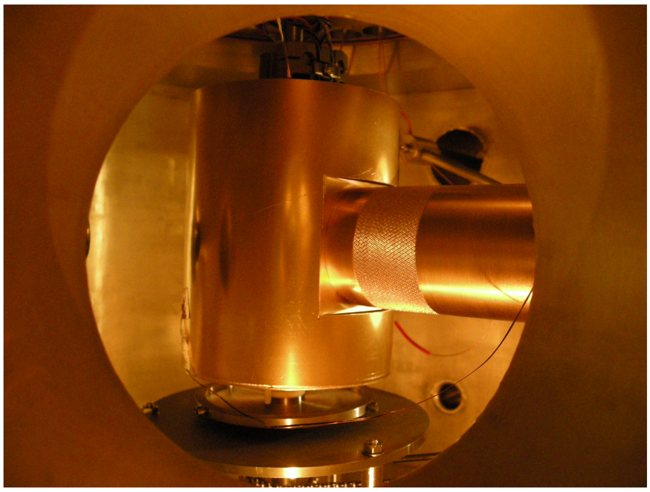

(d) Connecting shielding path

Figure 5.8: Installation

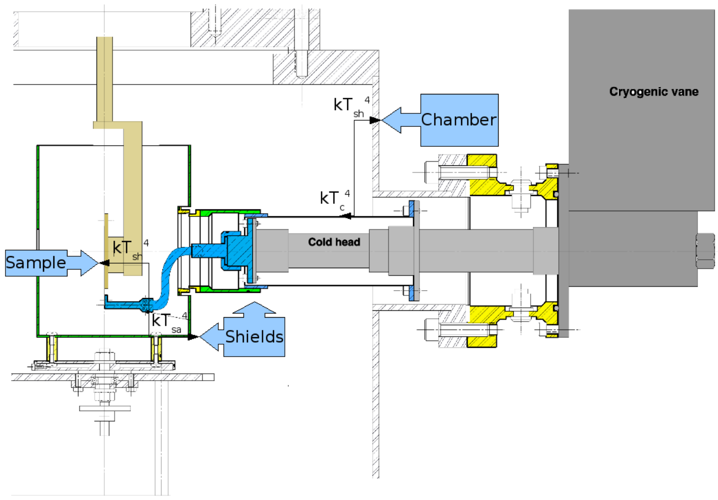

Figure 5.9: The actual experimental setup with radiation flux

Chapter 6

Tests and calibration

There is a significant separation between the diode that controls the temperature of the sample and the heater resistance located in the cold-finger. Therefore there is an unavoidable temperature gradient between them which means that the sample temperature must be evaluated through calibration on the basis of the temperature of the cold-finger.

In order to determine the lowest stable sample temperature values, the next plot shows the lowering of the temperature as a function of time without using the heater installed in the cold-finger.

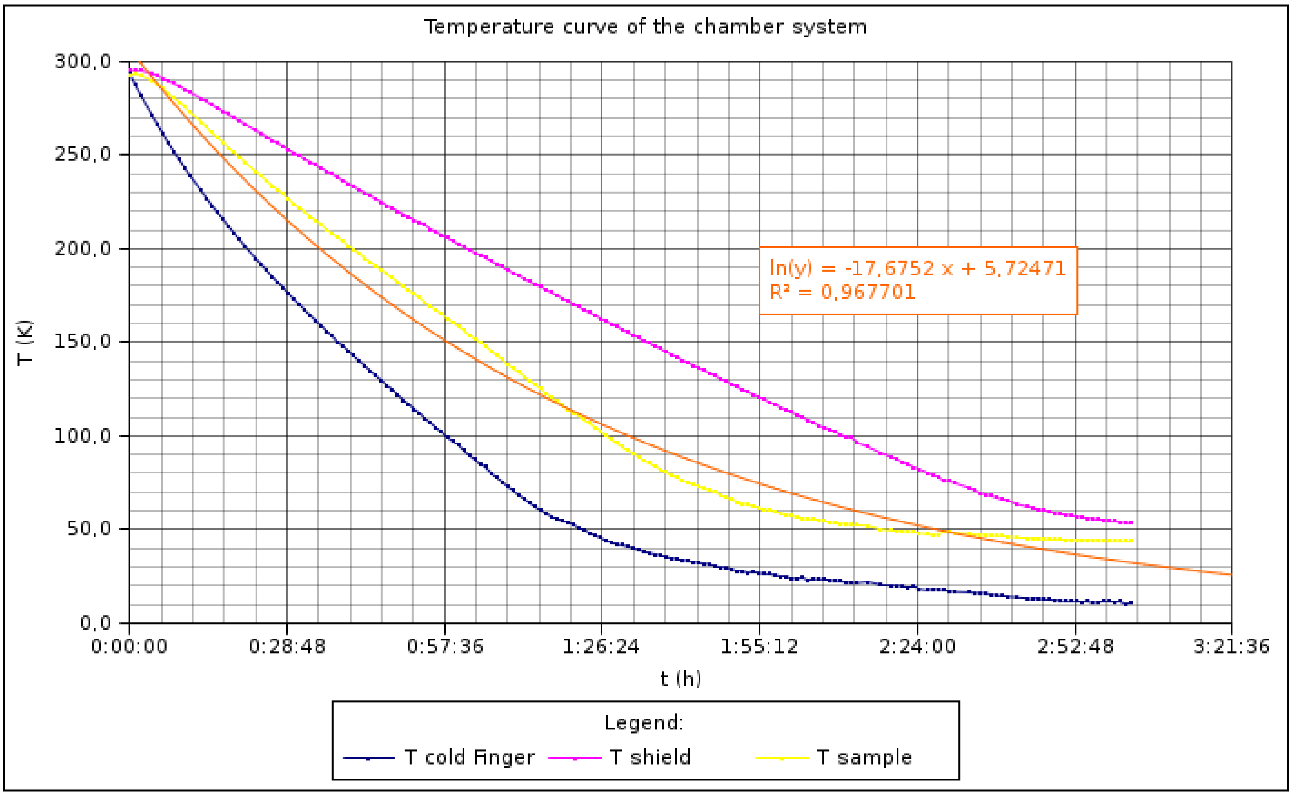

Figure 6.1: Temperature curve for the cold-finger, shield and sample as function of time

The calibration of the temperature is than obtained by setting the set point of the heater controller to a defined temperature and waiting 10 minutes for the stabilization of temperature. The values obtained are plotted in the fig.7.2

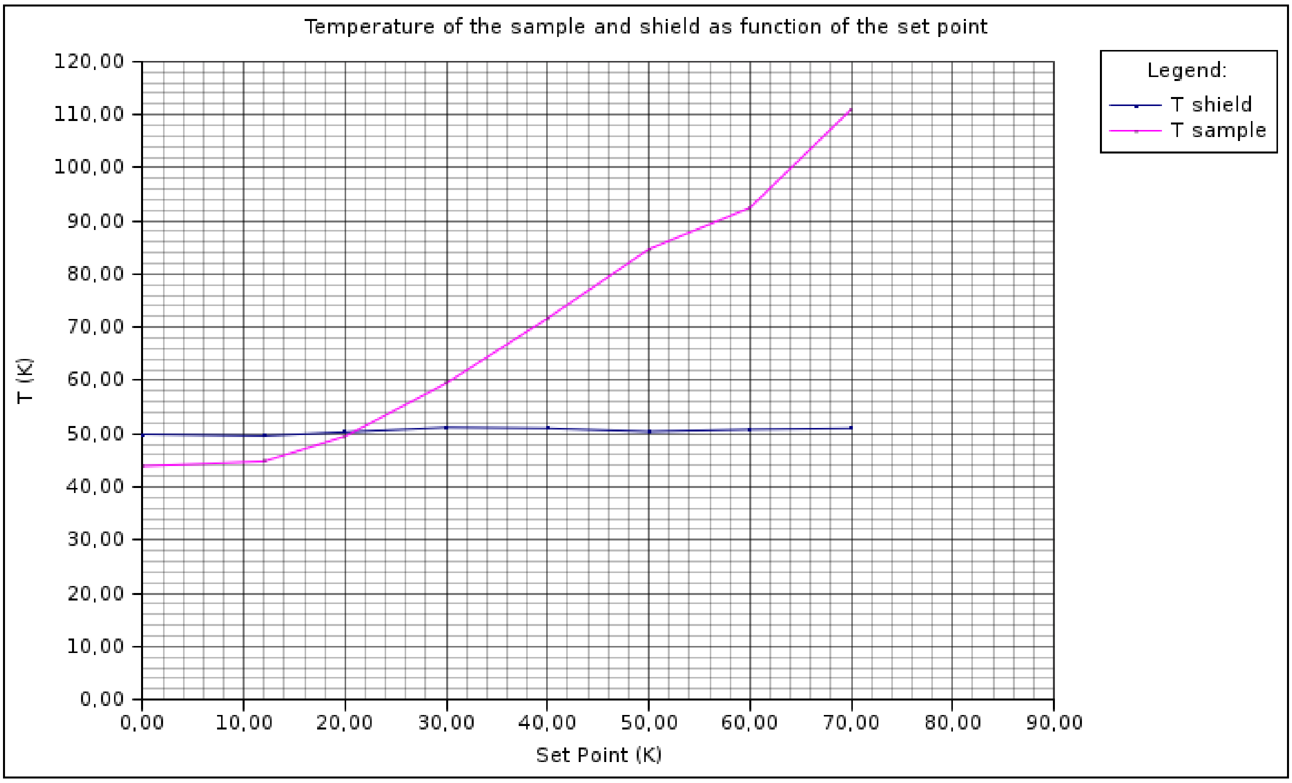

Figure 6.2: Temperature curve for the sample as function of the set point in the cold-finger heater controller

Clearly the shield suffers no influence of the conduction path, which is good. It keeps working as a condensation area avoiding the condensation on the sample.

The goniometer has an annealing block installed that provides a controlled (by an external controller) heating of its sample holder. Using this heater to control the sample temperature the calibration of the set point on the goniometer heater controller for the temperature in the sample is easier and more stable. The only limitation is that the calibration is referent to a specific goniometer.

The station as already been used for emission channeling at low temperature. The patterns acquired are not studied yet, but seem to show several differences. With This setup, we intend to study the local vibrations of atoms for each direction, measuring its anisotropy. It was a small step for the chamber, but a huge step for emission channeling and who knows what new physics it will provide.

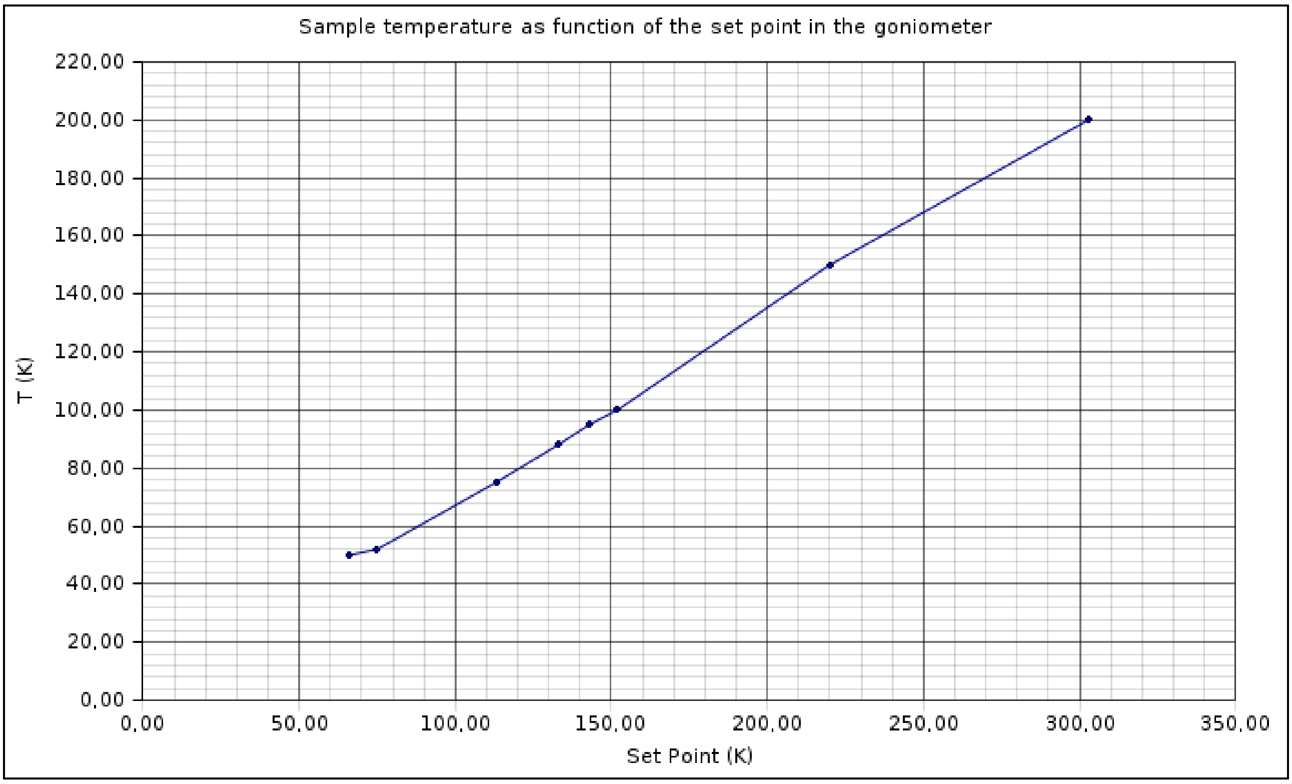

Figure 6.3: Temperature curve for the sample as function of the set point in the goniometer heater controller

Appendix A

Emissivity Factor

- Small Body (1) enclosed by much larger surface (2): $F_1 = \varepsilon_1$
- Infinite parallel flat plates: $\frac{1}{F_{1\ 2}=\frac{1}{\varepsilon_1}+\frac{1}{\varepsilon_2}-1}$
- Long concentric cylinders or spheres: $\frac{1}{F_{1\ 2}} = \frac{1}{\varepsilon_1} + \frac{A_1}{A_2}\left(\frac{1}{\varepsilon_2} - 1\right)$
- Gray surfaces connected by a reradiating nonconducting surface:

$$\frac{1}{F_{1\ 2}F_{conf.}} = \frac{1}{\varepsilon_1} - 1 + \frac{A_1}{A_2}\left(\frac{1}{\varepsilon_2} - 1\right) + \frac{1+\frac{A_1}{A_2}(1-2F_{conf.})}{1-\frac{A_1}{A_2}F_{conf.}^2}$$

Material	Emissivity (ε_n) at different temperatures (K)							
	100	200	300	400	600	800	1000	1200
Highly polished Aluminum	0.02	0.03	0.04	0.05	0.06			
Anodized Aluminum			0.82	0.76				
Highly Polished Copper			0.03	0.03	0.04	0.04	0.04	
Stably Oxidized Copper					0.50	0.58	0.80	
Highly Polished Gold	0.01	0.02	0.03	0.03	0.04	0.05	0.06	
Polished Silver			0.02	0.02	0.03	0.05	0.08	
Polished Stainless Steel			0.17	0.17	0.19	0.23	0.30	
Highly Oxidized Stainless Steel						0.67	0.70	0.76

Table A.1: Emissivity

Appendix B

Conductivity

Material	Thermal Conductivity (Wm^1K^1) at different temperatures (K)							
	100	200	400	600	800	1000	1200	1500
Pure Aluminum	302	237	240	23	218			
Aluminum oxide	450	82	32.4	18.9	13.0	10.5		
Alloy 2024-T6	65	163	186	186				
Alloy 195, Cast			174	185				
Pure Copper	482	413	393	379	366	352	339	
Commercial Bronze		42	52	59				
Gold	327	323	311	298	284	270	255	
Pure Iron	134	94.0	69.5	54.7	43.3	32.8	28.3	32.1
Armco Iron	95.6	80.6	65.7	53.1	42.2	32.3	28.7	31.4
Carbon steel AISI 1010			56.7	48.0	39.2	30.0		
Stainless Steel AISI 302			17.3	20.0	22.8	25.4		
Stainless Steel AISI 304	9.2	12.6	16.6	19.8	22.6	25.4	28.0	31.7
Stainless Steel AISI 316			15.2	18.3	21.3	24.2		
Stainless Steel AISI 347			15.8	18.9	21.9	24.7		
Lead	39.7	36.7	34.0	31.4				
Pure Nickel	164	107	80.2	65.6	67.6	71.8	76.2	82.6
Silver	444	430	425	412	396	379	361	
Tin	85.2	73.3	62.2					

Table B.1: Thermal Conductivity

Material	R with $10^2 kN/m^2$ contact pressure	R with $10^4 kN/m^2$ contact pressure
Stainless steel	6-25	0.7-4.0
Copper	1-10	0.1-0.5
Magnesium	1.5-3.5	0.2-0.4
Aluminum	1.5-5.0	0.2-0.4

Table B.2: Contact resistance in vacuum

Bibliography

[1] Ulrich Whal, “Emission channeling:charged particle-solid interaction, detection and lattice location methods” , Instituto Tecnológico e Nuclear, Submitted to the University of Lisbon as part of the process of “Agregação”.

[2] Manuel Ribeiro da Sílva, “Tutorial de técnicas de Vácuo Física e Técnologia“, centro de física nuclear.

[3] Randall F. Baron, “Cryogeni Heat Transfer“, 1999 Taylor & Francis.

[4] web page on the concept of the refrigerator, http://en.wikipedia.org/wiki/Refrigerator.

[5] Frank P. Incropera & David P. De Witt, “Fundamentals Of Heat and Mass Transfer“.